Synthesis and Interfacial Behavior of Amphiphilic Hyperbranched Polymers: Poly(ethylene oxide)−Polystyrene Hyperbranches

S. Peleshanko,[†] R. Gunawidjaja,[†] S. Petrash,[‡] and V. V. Tsukruk*,[†]

Department of Materials Science and Engineering, Iowa State University, Ames, Iowa 50011, and Corporate Researches, National Starch and Chemical Company, Bridgewater, New Jersey 08807

Received February 28, 2006; Revised Manuscript Received May 4, 2006

ABSTRACT: We report the synthesis of novel hyperbranched amphiphilic poly(ethylene oxide)−polystyrene (PEO−PS)$_n$ copolymers obtained by controlled radical polymerizations: nitroxide mediated polymerization (NMP) and reversible addition−fragmentation chain transfer (RAFT). The macroinimers used to synthesize copolymers have the general structure AB*, where A stands for PEO with a terminal double bond and B* stands for a PS block with a terminal initiating group (TEMPO or RAFT CTA). Bulk NMP yielded copolymers with higher molecular weight and higher polydispersity. RAFT polymerization in solution gave hyperbranched copolymers with higher molecular weight but lower polydispersity. Langmuir monolayers displayed reversible amphiphilic behavior at the air−water interface. The random, mixed character of short hydrophilic and hydrophobic fragments results in peculiar surface behavior: unlike regular linear and star block copolymers, the amphiphilic hyperbranched macromolecules with higher PEO content are spread at the air−water interface and short PEO fragments are not submerged into the water subphase even at high compression.

Introduction

Recent results on highly branched polymers with different chemical compositions and architectures demonstrated that the presence of joints and branches, treelike architecture, and a low level of entanglements leads to significant modification of physical properties in comparison with their linear counterparts.[1,2] Polymers with a small but controllable number of branches are also of interest because such materials may offer a practical method to more efficient control of the physical properties by waiving chemical composition and architecture. Dendrimers, hyperbranched and dendritic macromolecules with their fractal structure and multitude of branches, have attracted the most attention in this field.[3−6] However, a large-scale industrial application of regular dendrimers, such as for drug delivery and as catalytic systems, is limited by several factors, most importantly the cost in synthesis and purification.[7]

Hyperbranched molecules possess the treelike structure similar to that of dendrimers with the same known benefits in properties, accompanied by reduced cost and time of synthesis compared to dendrimers. Often, these molecules are created in one-pot synthesis without the lengthy stages of stepwise reaction and purification necessary with traditional dendrimers. Although significant polydispersity and inherent defects of their chemical structure caused by internal cyclization and side reactions, hyperbranched polymers possess, to a great extent, similar characteristics of compact nanoparticle-like structures with a significant fraction of terminal groups located on the exterior of the molecules.[10−14] However, in contrast to highly regular dendrimers, hyperbranched polymers do not show sharp transitions and exhibit a macroscopic spreading behavior.[15] Despite their irregular chemical structures, introducing multiple weak intermolecular interactions such as hydrogen bonding can facilitate their assembly into well-ordered one-dimensional microscopic or even macroscopic fibrils.[8] Amphiphilic branched

copolymers with hydrophilic and hydrophobic segments have been the subject of numerous studies.[9,10] In particular, branched macromolecules containing hydrophilic PEO segments and hydrophobic segments, such as PS, have attracted much attention, because PEO segments are not only hydrophilic but also nonionic and crystalline. The amphiphilic nature of these copolymers containing dissimilar segments gives rise to special properties in selective solvents, at surfaces, as well as in the bulk, owing to microphase separation.[11]

Novel macromolecular architectures such as highly branched and star-shaped block copolymers have been found to exhibit peculiar aggregation behavior,[12−15] which can be used for interesting developments such as a guided formation of fluorescent nano- and microfibers as well as metal nanoparticles.[16,17] Due to multifunctionality of the multiple terminal groups complex intra- and intermolecular interactions should be considered for understanding their assembly in solution, surfaces, and interfaces.[18−25] Unique morphologies were found in branched and star block copolymers that are not observed for linear block copolymers.[26−29] At the air−water interface, the behavior of star-shaped copolymer is qualitatively identical to linear systems; the hydrophobic chain collapses into globules while hydrophilic chain spreads out to form pancake structure.[30−33] However, at high surface pressure, recent studies have shown that the crowding of hydrophobic PS chains at a single junction point in asymmetric heteroarm PEO-*b*-PS$_m$ star polymers resulted in increasing circular micellar stability.[34,35]

It has been suggested that hyperbranched polymers can be applied as functionalized cores for the assembly of star molecules. Kim and Webster[36] described the use of modified hyperbranched poly(phenylenes) as macroinitiators for the synthesis of star polymers by anionic polymerization, although with limited success, due to a low conversion of the end groups into initiating sites and low stability of the macroinitiator. Recently, other polymerization techniques have been presented based on the idea of modifying branched molecules by the "grafting from" method. Promising results were obtained by free radical polymerization based on hyperbranched polymeric azo initiators[37] and living radical polymerization.[38] In addition, Gauthier et al.[39] described the successful preparation of am-

* To whom correspondence should be addressed. E-mail: vladimir@iastate.edu.
† Department of Materials Science and Engineering, Iowa State University.
‡ Corporate Researches, National Starch and Chemical Company.

phiphilic arborescent graft copolymers with a poly(ethylene oxide) shell via the "grafting from" method. Voit et al[40] presented a new multifunctional hyperbranched macroinitiator prepared by a one-step modification of terminal reactive groups into initiating moieties. The hyperbranched macroinitiator was suitable for the polymerization of 2-oxazoline monomers by a cationic ring opening mechanism which provides an excellent methodology for the synthesis of graft or block copolymers.[41]

Hyperbranched polymers require a relatively narrow polydispersity (<1.3) in order to prepare well-defined multiarm star polymers. Frey et al. reported a strategy for controlled preparation of the hyperbranched polyglycerol (PG) with narrow polydispersity via ring-opening multibranching polymerization.[42] In another work, the same group demonstrated that the solubility and flexibility of these polyether polyols can be tailored by the attachment of oligo(propylene oxide) segments,[43] leaving the functionality unchanged. On the basis of these initiator-cores, poly(ethylene oxide) stars with up to 55 PEO chains and low polydispersity (M_w/M_n < 1.5)[44] and poly(methyl acrylate)[45] multiarm star polymers have been prepared.

Self-condensing vinyl polymerization (SVCP) introduced by Frechet[38] has been applied in the synthesis of a variety of the functionalized hyperbranched polymers.[46] Initiator-monomers ('inimers') have general structure AB*, where A stands for double bond and B* for an initiating groups. Another approach involved the SCVP of a macromonomer that has both an initiator at one terminal and a polymerizable group at the other, via atom transfer radical polymerization (ATRP)[47,48] and SmI$_2$-induced transformation.[49] Unfortunately, for most of the hyperbranched polymers prepared via SCVP, their dendritic parts consist of only one kind of polymer segment. Therefore, this approach has been extended to the controllable copolymerization of a vinyl monomer M with "inimers" AB*,[50,51] which led to the random branched copolymers. RAFT polymerization has been shown to be excellent tool for producing hyperbranched polymers in one-pot with narrow polydispersity.[52] It is also allowed the introduction of a variety of end group functionalities on the final polymers, which could lead to new type of behavior.[53]

Considering that, to the best of our knowledge, no attempts have been made to synthesis amphiphilic hyperbranched copolymers from classical hydrophilic and hydrophobic segments of PEO and PS, we focus on the synthesis of the novel amphiphilic hyperbranched (PEO−PS)$_n$ copolymers with controlled chemical composition. The methods described above cannot be applied to the PEO−PS block copolymers, so we developed a new strategy for the synthesis of the (PEO−PS)$_n$ hyperbranched polymers. These hyperbranched copolymers possess the same length of the PEO blocks and different lengths of the PS chains. In this study, we focus on the investigation of amphiphilic hyperbranched (PEO−PS)$_n$ copolymers synthesized under different conditions by controlled radical polymerization. We report on the interfacial behavior of amphiphilic hyperbranched copolymers at the air−water interface, surface morphology, and film microstructure on a solid substrate.

Experimental Procedures

Chemicals. Tetrahydrofuran (THF) was purified by drying over sodium-benzophenone before distillation. Styrene (St) was stored over calcium hydride and then vacuum distilled before use. Methylene chloride, triethylamine (TEA) and *N,N,N′,N″,N″*-pentamethyldiethylenetriamine (PMDETA) were distilled over CaH$_2$. Copper(I) bromide (CuBr) was purified according to a reported procedure.[54] *S*-1-dodecyl-*S′*-(α,α′-dimethyl-α″-acetic acid)trithiocarbonate was synthesized according to the literature.[55] 2,2′-Bipyridine (Bipy, Acros), 1-(benzyloxymethyl)tri(ethylene glycol)

(Aldrich), 2-bromopropionyl bromide (Alfa Aesar), 2,2,6,6-tetramethylpiperidine 1-oxyl (TEMPO, Aldrich), *tert*-butyldimethylchlorosilane (TBS−Cl, 1 M solution in THF, Aldrich), tetrabutylammonium fluoride (TBAF, 1 M solution in THF, Aldrich) and 4-(dimethylamino)pyridine (DMAP, Acros) were used as received.
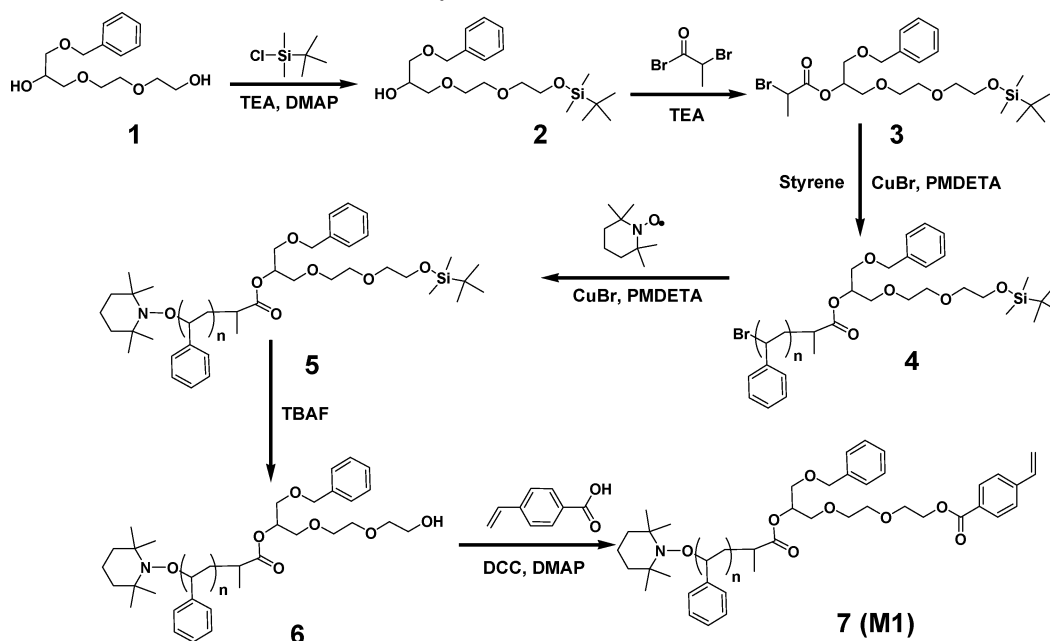
Synthesis of PEO−PS Macroinitiator M1. Synthesis of 2. Dry triethylamine (3.2 mL, 1.2 equiv) and a catalytic amount of (dimethylamino)pyridine (0.1 g, 0.04 equiv) were added to a solution of 1-(benzyloxymethyl)tri(ethylene glycol) (**1**) (5.4 g, 20 mmol) in 50 mL of dry THF. TBS−Cl (22.0 mL, 1.1 equiv) was added, and the mixture was stirred for 24 h at room temperature. After filtration, the mixture was concentrated to yield a transparent orange liquid. The crude product was purified by column chromatography on silica gel with dichloromethane/acetone (9:1) to yield **2** as a transparent colorless liquid (4.8 g, 76.0% yield). ^{1}H NMR (CDCl$_3$, δ): 0.06 (s, 6H, −Si−C*H$_3$*), 0.89 (s, 9H, −Si−C(C*H$_3$*)$_3$), 2.71 (s, 1H, −CH−O*H*), 3.41−3.54 (m, 10H, −C*H$_2$*O−), 3.72−3.69 (t, 2H, −CH−C*H$_2$*O−CH$_2$−C$_6$H$_5$), 4.01 (m, 1H, −C*H*−OH), 4.52 (s, 2H, −O−C*H$_2$*−C$_6$H$_5$), 7.32 (m, 5H, −C$_6$*H$_5$*).

Synthesis of 3. A 3.84 g (10 mmol, 1 equiv) sample of **2** was dissolved under an argon atmosphere in a solution of 1.5 mL of TEA in 75 mL of anhydrous THF. After this, 1.2 mL (1.1 equiv) of 2-bromopropionyl bromide was added dropwise at 0 °C (ice bath) over 15 min with vigorous stirring. The mixture was then stirred overnight at room temperature. The triethylamine hydrobromide was precipitated, and after filtration, the solution was concentrated by evaporation. The crude product was purified by column chromatography on silica gel with dichloromethane/acetone (9:1) to yield **3** as a transparent colorless liquid (4.4 g, 84.6% yield). ^{1}H NMR (CDCl$_3$, δ): 0.06 (s, 6H, −Si−C*H$_3$*), 0.9 (s, 9H, −Si−C(C*H$_3$*)$_3$), 1.72 (d, 3H, −CH(Br)−C*H$_3$*), 3.35−3.9 (m, 12H, −C*H$_2$*O−), 4.4 (m, 1H, −C*H*(Br)−CH$_3$), 4.51 (s, 2H, −O−C*H$_2$*−C$_6$H$_5$), 5.22 (m, 1H, −C*H*−OCO−CH(Br)−CH$_3$), 7.32 (m, 5H, −C$_6$*H$_5$*).
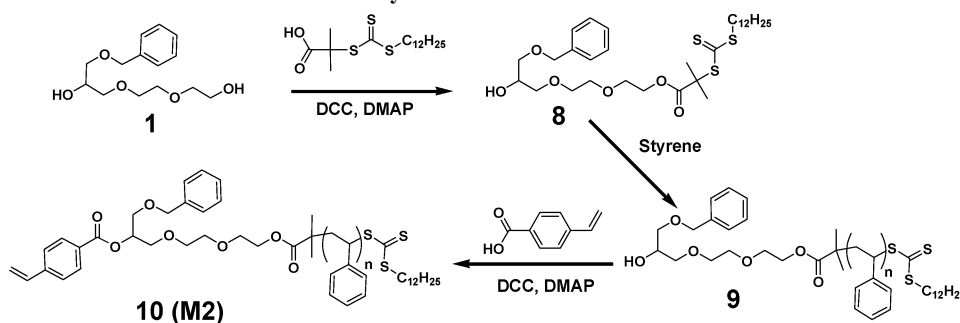
Synthesis of 4. ATRP of styrene using compound **3** as initiator was done according to the standard procedure: into a 10 mL round-bottom flask were added 0.52 g of **3** (1.0 mmol) and 28.4 mg of CuBr (0.2 mmol) in an oxygen-free atmosphere. The flask was sealed with a rubber septum and secured with copper wire. The sealed flask was frozen with liquid nitrogen, degassed by one freeze−pump−thaw cycle and backfilled with argon gas. Then, 2.06 g of styrene monomer (0.02 mol) was added via syringe. Finally, 34.3 mg of PMDETA (0.2 mmol,) was added into the solution mixture under stirring. Again, the contents of the flask was frozen and degassed with two more freeze−pump−thaw cycle before backfilling the flask with argon gas. The flask was then placed in a thermostatic bath at 90 °C under stirring for overnight. The next day, the contents had solidified. Once cooled, it was dissolved in dichloromethane and ran through alumina column to separate the polymer from copper bromide catalysts. Next, the polymer solution was concentrated and precipitated in methanol (yield ca. 85%). M_n-(GPC) = 2050 Da, PDI = 1.16. ^{1}H NMR (CDCl$_3$, δ): 0.05 (s, 6H, −Si−C*H$_3$*), 0.88 (s, 9H, −Si−C(C*H$_3$*)$_3$), 1.2−2.5 (m, −CH−C*H$_2$*− of PS and −C*H$_3$*), 3.35−3.9 (m, 12H, −C*H$_2$*O−), 4.4−4.55 (m, −C*H*(Br) and −O−C*H$_2$*−C$_6$H$_5$), 5.14 (m, 1H, −C*H*−OCO−CH−CH$_3$), 6.3−7.4 (m, 5H, −C$_6$*H$_5$*).

Synthesis of 5. The bromine functional group was substituted for TEMPO as follows: into a 5 mL round-bottom flask were added 0.86 g of **4** (0.42 mmol), 0.1 g of TEMPO radical (0.63 mmol), and 60.3 mg of CuBr (0.42 mmol) in an oxygen-free atmosphere. The flask was sealed with a rubber septum and secured with copper wire. The contents were frozen and degassed and underwent a freeze−pump−thaw cycle once before being backfilled with argon gas. Then 1 mL of distilled and degassed toluene was added, followed by addition of 72.8 mg of PMDETA (0.42 mmol) under stirring; both compounds were added via syringe under argon purge. The solution mixture was frozen and degassed with two more freeze−pump−thaw cycles before being placed overnight in a thermostated at 90 °C oil bath to give polymer **6**. The next day, the solution mixture was diluted in dichloromethane and ran through an alumina column using a mixture of dichloromethane and hexane

Scheme 1. Synthesis of the Macroinimer M1

Scheme 2. Synthesis of the Macroinimer M2

(1:9) as a solvent. Unreacted TEMPO radicals were removed first during the separation in the form of orange solution. Most of the polymer was washed out by dichloromethane, but a mixture of methanol and dichloromethane (2:8) solvent was used to completely remove compound **6** from the column (yield ca. 75%). M_n(GPC) = 2175 Da, PDI = 1.15. ^{1}H NMR (CDCl$_3$, δ): 0.05 (s, 6H, $-$Si$-$CH_3), 0.88 (s, 9H, $-$Si$-$C(CH_3)$_3$), 1.2$-$2.5 (m, $-$C$H-$CH$_2-$ of PS,$-$CH_3 and $-$CH_2 of TEMPO), 3.35$-$3.9 (m, 12H, $-$CH_2O$-$), 4.4 (s, $-$O$-$CH_2-C$_6$H$_5$), 5.14 (m, 1H, $-$C$H-$OCO$-$CH$-$CH$_3$), 6.3$-$7.4 (m, 5H, $-$C$_6$H$_5$).

Synthesis of 6. *tert*-Butyldimethylsilane (TBDMS) protecting group of compound **5** (545 mg, 0.25 mmol) was removed by treatment with 1 mL of 1 M tetrabutylammonium fluoride solution in THF diluted with another 5 mL of THF to give **5** after precipitation in methanol (yield ca. 75%).[56] M_n(GPC) = 2010 Da, PDI = 1.16. ^{1}H NMR (CDCl$_3$, δ): 1.2$-$2.5 (m, $-$C$H-$CH$_2-$ of PS,$-$CH_3 and $-$CH_2 of TEMPO), 3.35$-$3.9 (m, 12H, $-$CH_2O$-$), 4.4 (s, $-$O$-$CH_2-C$_6$H$_5$), 5.14 (m, 1H, $-$C$H-$OCO$-$CH$-$CH$_3$), 6.3$-$7.4 (m, 5H, $-$C$_6$H$_5$).

Synthesis of 7. 4-Vinylbenzoic acid (74 mg, 0.5 mmol), DMAP (15.8 mg, 0.13 mmol), and compound **6** (275 mg, 0.128 mmol) were added into a 15 mL round-bottom flask and dissolved in 8 mL of dry THF. The solution was cooled under stirring to 0 °C. After about 20 min, a solution of DCC (103 mg, 0.5 mmol) dissolved in 2 mL of dry THF was added into the flask. The solution mixture was allowed to warm to room-temperature overnight. After filtration, the solution was concentrated and precipitated twice in methanol (yield ca. 75%). M_n(GPC) = 2150 Da, PDI = 1.15. ^{1}H NMR (CDCl$_3$, δ): 0.05 (s, 6H, $-$Si$-$CH_3), 0.88 (s, 9H, $-$Si$-$C(CH_3)$_3$), 1.2$-$2.5 (m, $-$C$H-$CH$_2-$ of PS,$-$CH_3 and $-$CH_2 TEMPO), 3.35$-$3.9 (m, 12H, $-$CH_2O$-$), 4.4 (s, $-$O$-$CH_2-C$_6$H$_5$),

5.14 (m, 1H, $-$C$H-$OCO$-$CH$-$CH$_3$), 5.64 and 6.02 (m, 2H, $-$CH=CH_2), 6.3$-$7.4 (m, 5H, $-$C$_6$H$_5$), 7.45 and 8.00 (d, 4H, $-$C$_6$H$_4$).

Synthesis of PEO$-$PS Macroinitiator M2. Synthesis of 8. *S*-1-Dodecyl-*S'*-(α,α'-dimethyl-α''-acetic acid)trithiocarbonate (4.38 g, 12 mmol), DMAP (61 mg, 0.5 mmol), and 1-(benzyloxymethyl)-tri(ethylene glycol) (2.7 g, 10 mmol) were added into a 50 mL round-bottom flask and dissolved in 65 mL of dry THF. The solution was cooled under stirring at 0 °C. After about 20 min, a solution of 2.47 g (12 mmol) of DCC in 10 mL of dry THF was added into the flask. The solution mixture was allowed to stir overnight to room temperature. A white precipitate of urea was removed by filtration. After concentration, the crude product was purified by column chromatography on silica gel with ethyl acetate/hexane (3:7) to yield **8** as a transparent yellow viscous liquid (4.44 g, 72% yield). ^{1}H NMR (CDCl$_3$, δ): 0.85 (t, 3H, $-$CH$_2-$CH_3), 1.23 (m, 18H, $-$CH_2-), 1.65 (m, 2H, $-$S$-$CH_2-), (1.71 (s, 6H, $-$C(CH_3)$_2$), 2.63 (s, 1H, $-$CH$-$OH), 3.25 (t, 2H, $-$CH_2-OCO$-$C(CH$_3$)$_2-$), 3.21$-$3.64 (m, 12H, $-$CH_2O$-$), 4.00 (m, 1H, $-$C$H-$OH), 4.55 (s, 2H, $-$O$-$CH_2-C$_6$H$_5$), 7.30 (m, 5H, $-$C$_6$H$_5$).

Synthesis of 9. RAFT polymerization of styrene using compound **8** as initiator was done according to the standard procedure: into a 10 mL round-bottom flask were added 2.5 g (4.05 mmol) of **8**, 2 mL of hexane and 5 mL of styrene in an oxygen-free atmosphere. The sealed flask was frozen with liquid nitrogen, degassed by one freeze$-$pump$-$thaw cycle, and backfilled with argon gas. The flask was then placed in a thermostatic bath at 125 °C under stirring overnight. Once cooled, the product was dissolved in THF and purified by column chromatography on silica gel with ethyl acetate/hexane (2:8) to yield **9** as a transparent yellow viscous liquid (3.3 g, 48% conversion). M_n(GPC) = 1010 Da, PDI = 1.04. ^{1}H NMR

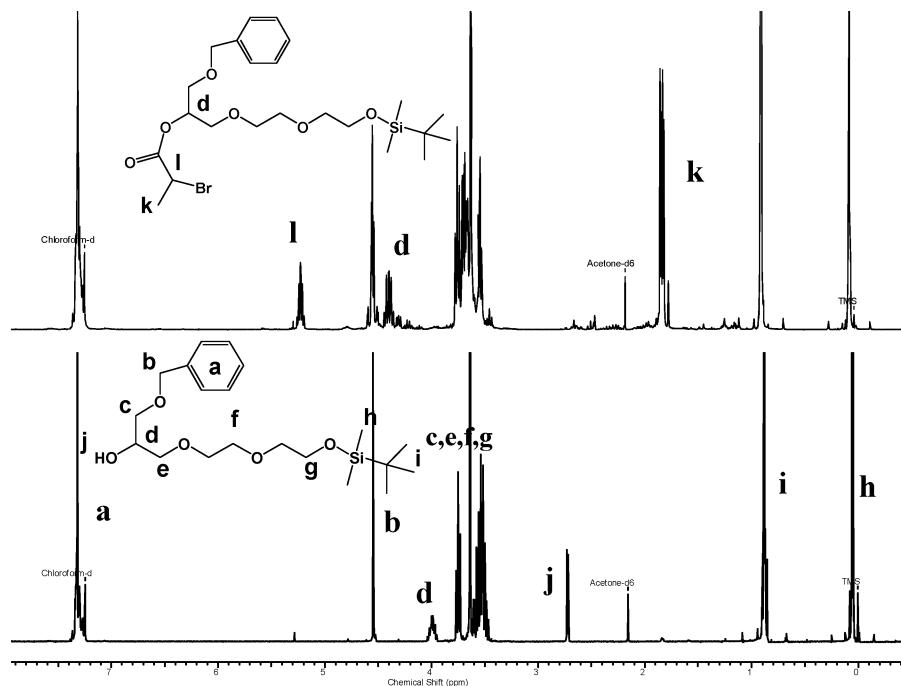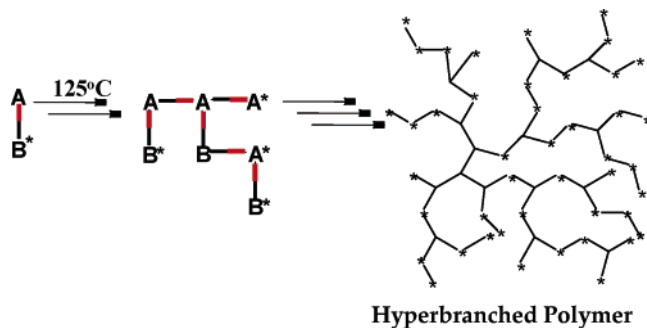**Figure 1.** ^{1}H NMR of compounds **2** and **3**.

Scheme 3. General Route of the Self-Condensing Vinyl Polymerization

Hyperbranched Polymer

(CDCl$_3$, δ): 0.85 (t, 3H, $-$CH$_2$$-CH_3$), 1.23 (m, 18H, $-$CH$_2$$-$), 1.35$-$2.75 (m, $-$CH$-$CH$_2$ of PS, and $-$S$-$CH$_2$$-$), (1.71 (s, 6H, $-$C(CH$_3$)$_2$), 2.63 (s, 1H, $-$CH$-$OH), 3.25 (t, 2H, $-$CH$_2$$-OCO-$C(CH$_3$)$_2$$-$), 3.23$-$3.65 (m, 12H, $-$CH$_2$O$-$), 4.02 (m, 1H, $-$CH$-$OH), 4.55 (s, 2H, $-$O$-$CH$_2$$-C_6H_5$), 6.35$-$7.45 (m, 5H, $-$C$_6$H$_5$).

Synthesis of 10. Macroinimer **M2** was synthesized from compound **8** in a manner similar to the procedure described above for compound **7**. Total yield was 80%. M_n(GPC) = 2150 Da, PDI = 1.04. ^{1}H NMR (CDCl$_3$, δ): 0.85 (t, 3H, $-$CH$_2$$-CH_3$), 1.23 (m, 18H, $-$CH$_2$$-$), 1.35$-$2.75 (m, $-$CH$-$CH$_2$ of PS, and $-$S$-$CH$_2$$-$), (1.71 (s, 6H, $-$C(CH$_3$)$_2$), 3.25 (t, 2H, $-$CH$_2$$-OCO-$C(CH$_3$)$_2$$-$), 3.23$-$3.65 (m, 12H, $-$CH$_2$O$-$), 4.92 (m, 1H, $-$CH$-$OCO$-$C$_6$H$_4$), 4.55 (s, 2H, $-$O$-$CH$_2$$-C_6H_5$), 5.44 and 5.75 (m, 2H, $-$CH$=$CH$_2$), 6.3$-$7.4 (m, 5H, $-$C$_6$H$_5$), 7.49 and 8.02 (d, 4H, $-$C$_6$H$_4$).

Synthesis of Hyperbranched Polymers. Self-condensing polymerization of the macromonomers was performed in bulk or in solution (60 wt % in DMF) at 125 °C according to a general route sketched in Scheme 3. Samples were taken at specific times using a degassed syringe and were dissolved in THF and the resulting solution kept in the freezer ($-$20 °C) prior to GPC analysis. Hyperbranched copolymers were heated with hexane (10 mL per 100 mg of the polymer) and then cooled to room temperature. A slightly yellow solution containing unreacted macromonomer along with low molecular weight fraction was removed. This procedure has been repeated additional two times.

Characterization. Monolayers were prepared from dilute chloroform solutions by the Langmuir technique on a KSV minitrough.[12]

The substrates for LB layers were polished silicon wafers (Semiconductor Processing Co.) of the {100} orientation. Wafers were cleaned according to an established procedure. ^{13}NMR spectra were obtained using a Varian VXR-300 system. The molecular weights and polydispersity of the star polymers were evaluated by gel permeation chromatography (GPC) in THF using Waters-GPC system equipped with a miniDawn (Wyatt Technology) light scattering detector. The X-ray measurements of bulk polymers were performed on a Rigaku Miniflex X-ray diffractometer. Scans were collected in the 2θ range from 1 to 40°, with a step of 0.02°, and a scan rate of 0.1° per minute. Monochromatic Cu Kα, radiation with a wavelength of 0.154 nm was used for all measurements. Surface morphology and microstructure of polymer layers were studied with a Dimension-3000 atomic force microscope in the tapping mode according to the usual procedure adapted in our lab.[57] Differential scanning calorimetry (DSC) was performed on an MDSC Q100 instrument with a heating rate of 20 °C/min in the range $-$60 to $-$125 °C. Approximately 2$-$5 mg of polymers was used for these measurements. The chemical structures of all molecules were illustarted with ChemDraw 8.0 software package. The molecular models of all molecules were built with the Materials Studio 3.0 software package by using the combination of molecular dynamics and energy minimization routines.

Result and Discussion

Synthesized Materials. 1-(Benzyloxymethyl)tri(ethylene glycol) (**1**) was chosen as a short PEO hydrophilic fragment due to affordable selective substitution of the primary hydroxyl group and convenient use of benzyl protons as a reference standard for calculating the molecular weight of polymers. In continuation of our previous work[34,35] on studying the effect of polymer structure on their surface properties, we synthesized two macroinimer with similar chemical compositions. According to ^{1}H NMR data, the RAFT and NMP initiating groups in hyperbranched copolymers presented here survived and can further initiate polymerization of a variety of monomers that can result in new highly branched functional star polymers.

The NMP synthetic route for the macroinimer is presented in Scheme 1. First, selective functionalization of the primary alcohol was conducted according to the well-established procedure by using DMAP as a catalyst (Figure 1, bottom).[58] Then,
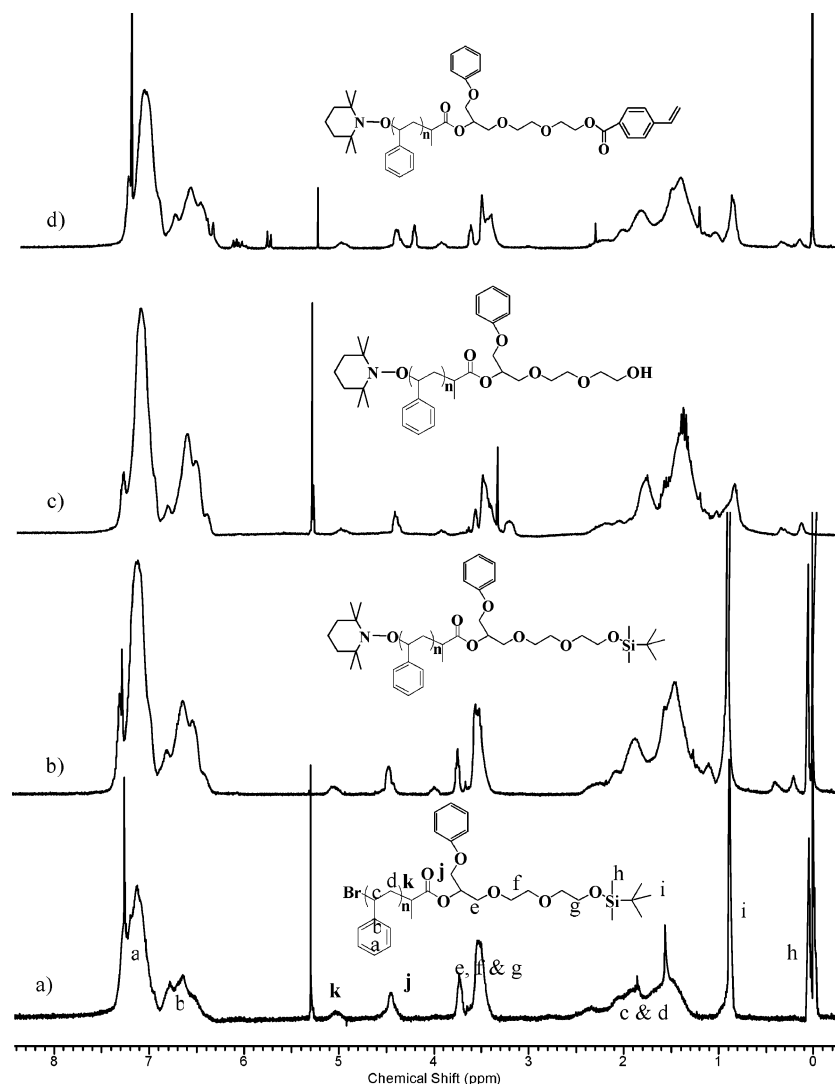
Figure 2. ^{1}H NMR of intermediates in the synthesis of the macroinimer **M1**.

a secondary alcohol group was modified by 2-bromopropionyl bromide to make polymer **3** suitable for the ATRP of the styrene (Figure 1, top). Polymerization of styrene was achieved in the presence of the 20% copper, catalyst which is known to produce polymers with low polydispersity (<1.1) and small molecular weight (<3000).[59] It had been shown that ATRP of the macroinimers has to be done in solution and with the presence of the catalyst. NMP in this case can be done either in bulk or solution without adding additional chemicals. The next step in synthesis of the macroinimer was the substitution of the bromine group in polymer **4** by TEMPO according to the literature procedure.[60,61] After removing the TBS protecting group, the hydroxyl group of polymer **6** was modified by 4-vinylbenzoic acid, which then finally resulted in polymer **7** (Scheme 1). For simplicity, we designate the final polymer **7** as macroinimer **M1**.

The ^{1}H NMR spectra and GPC of the intermediate TEG-PS polymers collected during end functionality transformations were used here for the illustration of controlled chemical step-by-step synthesis procedure implemented in this study (Figures 1 and 2). All characteristic peaks expected for the chemical groups of PEO and PS are clearly marked on this plot according to the literature values.[62] The appearance of the appropriate peaks for various functional groups at different stages of the synthetic procedure is indicated at these plots (Figures 1 and 2). The relative content of PEO and PS chains was calculated by

Table 1. Molecular Characteristics of the Macroinimers[a]

		GPC		NMR				
name	sample	M_n	PDI	N(EO)	N(St)	M_n	φ^a	φ^{total}
M1	TEG−PS−TEMPO	2175	1.15	3	12	1923	0.11	0.08
M2	TEG−PS−RAFT	1150	1.05	3	5	1284	0.22	0.12

[a] $\varphi^a = M_n(TEG)/M_n(PS)$ and $\varphi^{total} = M_n(TEG)/M_n(NMR)$ are volume fractions of the TEG fragments in macroinimers with and without alkyl tails. $M_n(TEG) = 150$, $M_n(PS) = N(St) \times 104$, and $M_n(NMR)$ is total molecular weight from NMR data.

Table 2. Chemical and Physical Characteristics of the Hyperbranched Copolymers

		before purification		after purification				
		GPC		GPC		LS		
poly-mer	sample	M_n	PDI	M_n	PDI	M_n	PDI	T_g, °C
P1	TEG−PS (bulk)	6400	11.5	7050	4.2	N/A[a]	N/A	45
P2	TEG−PS (DMF)	4160	5.2	6040	1.9	16 880	2.02	62
P3	TEG−PS−RAFT	6340	4.01	12 580	2.3	15 960	1.83	55

[a] The data interpretation is ambiguous due to the presence of additives.

integrating the aromatic signals for the PS backbone and a singlet signal at 4.4−4.5 ppm which is related to the methylene protons of the benzyl-protecting group. The calculated parameters for the chemical composition of the macroinimer **M1** from NMR data are presented in Table 1. From the NMR data we concluded that the number of styrene units was 12 for the TEMPO-terminated macroinimer (Table 1, Figure 2).
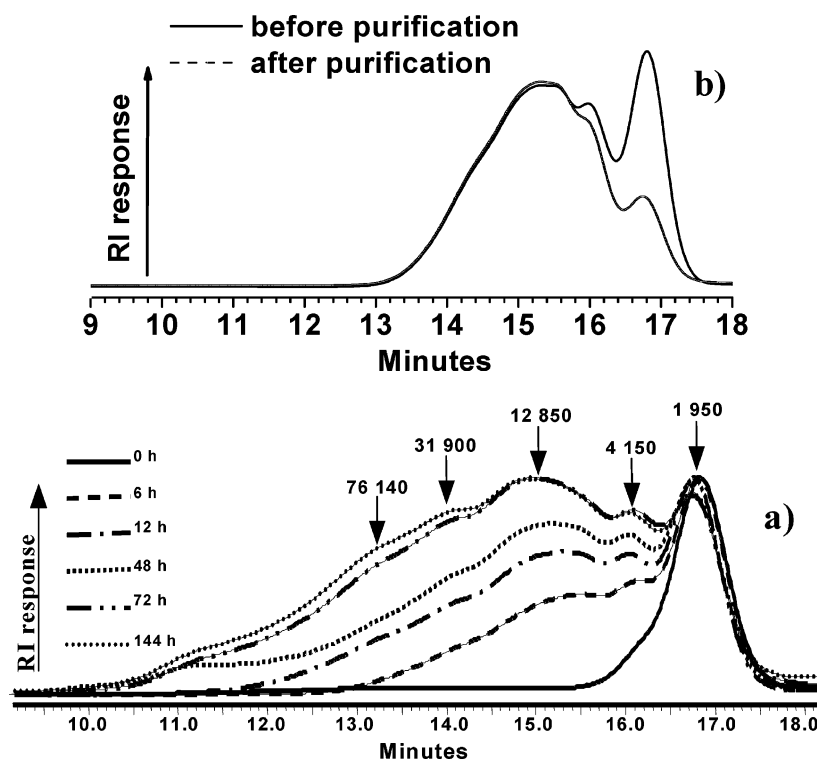
Figure 3. GPC traces of the polymerization of **M1** in bulk at 125 °C (a) and hyperbranched polymer **P2** before and after purification (b). Peak values were calculated using PS calibration curve.

After the synthesis of macroinimer **M1**, the next logical step was to check the effect of the polymerization conditions on the molecular characteristics of the hyperbranched copolymers. Hyperbranched copolymers were prepared by SCVP of the macroinimers in bulk or in solution and resulted in hyperbranched polymers with different molecular characteristics (Table 2). The progress in synthesis of the hyperbranched copolymers by NMP in bulk and solution and the quality of the final molecular weight distribution were monitored by GPC (Figure 3, Tables 2). GPC traces of kinetic samples taken from NMP polymerization of **M1** are illustrated in Figure 3. As expected, the polymer obtained by polymerization in bulk possessed a very wide molecular weight distribution (PDI > 11). The asymmetric shape of the GPC traces and overlapped peaks may be explained by the increasing difference in molecular weights of the hyperbranched copolymer fractions. It can be related to different grafting rates due to the decreasing mobility of macroinimers caused by increasing intrinsic viscosity of copolymers with polymerization time.[63] The difficulty observed for the macroinimer to meet a reactive group in the polymacroinimer due to the steric constrains caused coupling between macromolecules (Figure 3a). However, as it has been shown previously for the self-condensing vinyl polymerizations of the AB* inimers, distinct peaks of the dimer, tetramer, etc. were observed at every stage of the polymerization.[46] It is worth noting that no cross-linked polymer has been observed after 144 h.

Polymerization of the macroinimer **M1** in solution dramatically decreased the degree of polymerization and lowered the PDI to 4−5 (Figure 3b, Table 2). Additional purification of the hyperbranched copolymers by selective extraction using hexane further lowered the PDI (Figure 3b, Table 2), but still small amount of unreacted macroinimer could not be removed. GPC analysis revealed the degree of polymerization of ca. 3 units for the NMP in bulk and solution (Table 1). Chemical composition of the hyperbranched polymers **P1** and **P2** was

confirmed by NMR data (Figure 4). The ^{1}H NMR spectra of the purified polymers showed signals of both fragments, TEG and PS, and the complete disappearance of vinyl end groups. Despite significant variation in molecular characteristics, there is no considerable difference in NMR spectra of **P1** and **P2** hyperbranched polymers, indicating very similar chemical compositions (Table 2).

To get hyperbranched copolymers with higher molecular weight, a new macroinimer with lower molecular weight was synthesized. The synthetic route of the macroinimer for the RAFT polymerization is presented in Scheme 2. First, selective functionalization of the primary alcohol was conducted according to the well-established procedure by using DMAP as a catalyst.[64] Polymerization of styrene was achieved at 125 °C which leads to the polymers with low polydispersity (<1.1) and small molecular weight (<1500 Da). Then the secondary alcohol group of the polymer **9** was modified by 4-vinylbenzoic acid resulted final polymer **10** (Scheme 2, Figure 5). For simplicity, we designate final polymer **10** as macroinimer **M2**. From NMR data, we concluded that the number of styrene units was 5 for the RAFT CTA-terminated macroinimer **M2** (Table 1, Figure 5).

RAFT polymerization of the **M2** in DMF solution led to the hyperbranched copolymers with relatively low polydispersity after purification with a symmetrical shape in GPC traces (Figure 6, Table 2). The residual amount of the linear macroinimer presented in the polymerization system even after 96 h may be explained by two factors: one factor is related to the RAFT mechanism itself,[65] which causes slow consumption of the linear macroinimer. The second factor may be related to the nature of the solvent. In our case, DMF is known to undergo H-subtraction and form radicals, which may interfere with the polymerization.[66] Chemical composition of the **P3** hyperbranched polymer was confirmed by ^{1}H NMR data (see peak assignments above) (Figure 7).
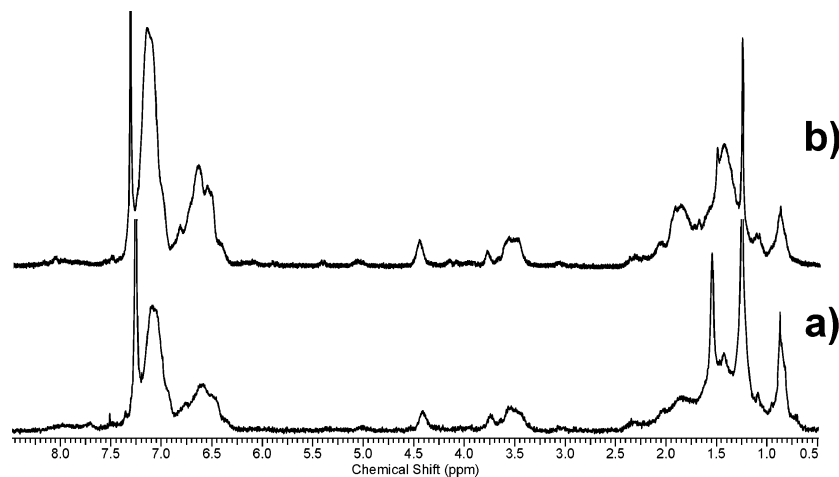
Figure 4. ^{1}H NMR of hyperbranched polymers **P1** (a) and **P2** (b).
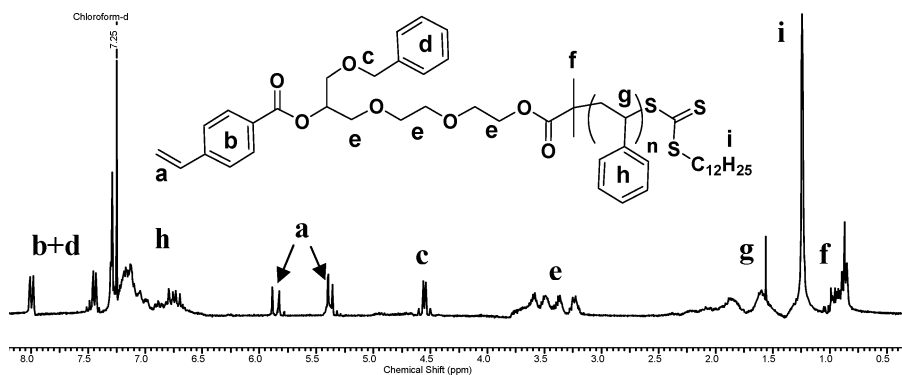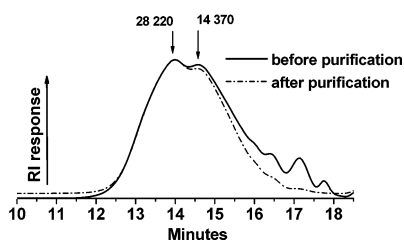

Figure 5. ^{1}H NMR of the macroinimer **M2**.

Figure 6. GPC traces of the **P3** polymer before purification (solid) and after purification (dash). Peak values were calculated using PS calibration curve.

As is known, the absolute value of the molecular weight cannot be directly determined from GPC because of the specific solution properties caused by nonlinear architecture of the polymer chains.[67] Thus, light scattering data have been used to get more reliable estimation of the molecular weight giving the much higher value between 16000 and 18000 Da and polydispersity similar to that measured by GPC (Table 2). The difference between GPC and LS data usually observed for highly branched polymers is due to the different conformational states and interactions of star polymers as compared to linear chains for PS calibration standards.[68] Light scattering data for **P1** could be not treated unambiguously due to, probably, the presence of un-removable additives.

Because of the overlapping peaks in ^{1}H NMR data for relatively high molecular weights, it is virtually impossible to calculate the degree of branching (DB) of the hyperbranched polymers. Therefore, we assumed that according to Müller's theoretical predictions, the DB of a polymacroinimer can reach 0.465 for limiting cases, when all double bonds are fully converted.[63] Considering the uncertainty of this parameter, two limiting cases in the architecture of the copolymers should be

considered: brush/comblike structure and truly hyperbranched structure (Scheme 4). Because of the limitation of the modeling software, we presented chemical structure of **P3** polymer containing only 6 monomeric units, but 11 for the corresponding 3D molecular models. The chemical structures and molecular models visualizing space distribution of two different blocks in molecules with different chemical compositions presented in Scheme 4 show that in the former case, a highly asymmetrical molecular structure is expected unlike the later case with a widely spread network of chemically connected fragments.

Characterization in the Bulk State. X-ray data for the hyperbranched (PEO−PS)$_n$ copolymers clearly demonstrated the amorphous structure of these copolymers at room temperature (Figure 8). Sharp peaks in a wide-angle region indicating the presence of the PEO crystalline phase were not detected for any of the polymers and monomers studied (occasional sharp peaks observed are due to unremovable organic species). Apparently, the presence of short PEO blocks (only 3 EO units, Table 1) attached to the PS block in a combination with random branching inhibited PEO crystallization. Accordingly, DSC curves showed only glass transition temperature in the low range of 45−62 °C which is due to the smaller PS segments having a much lower T_g (Table 2).

Surface Morphology. The reproducible and reversible $\pi−A$ isotherms were obtained for all hyperbranched compounds and macroinimers synthesized here (Figure 9). This surface behavior indicates the formation of a stable Langmuir monolayer with liquid and solid 2D phase sequences typical for amphiphilic compounds.[69] The isotherms for macroinimers showed increased surface pressure for surface areas per molecule below 0.9 nm^2 which is expected for the given chemical composition with PS chains controlling the condensed state. The surface area per
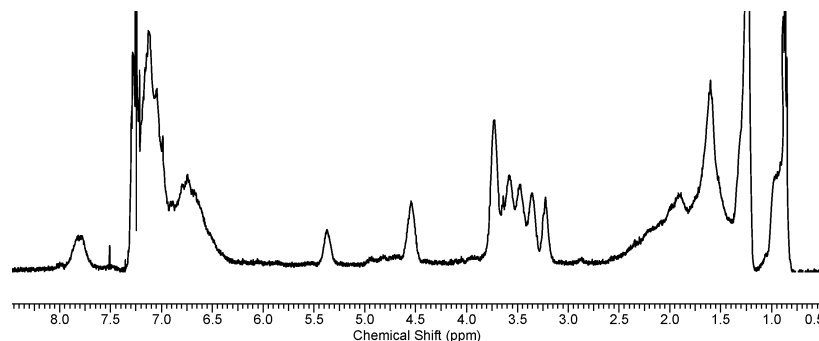
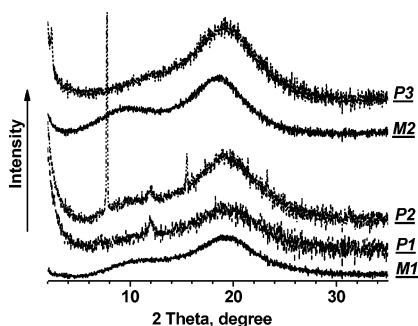**Figure 7.** ¹H NMR of hyperbranched polymers **P3**.

Figure 8. X-ray diffraction data of the macroinimers and corresponded hyperbranched polymers. Sharp peaks are due to the presence of un-removable organic impurities in polymers.
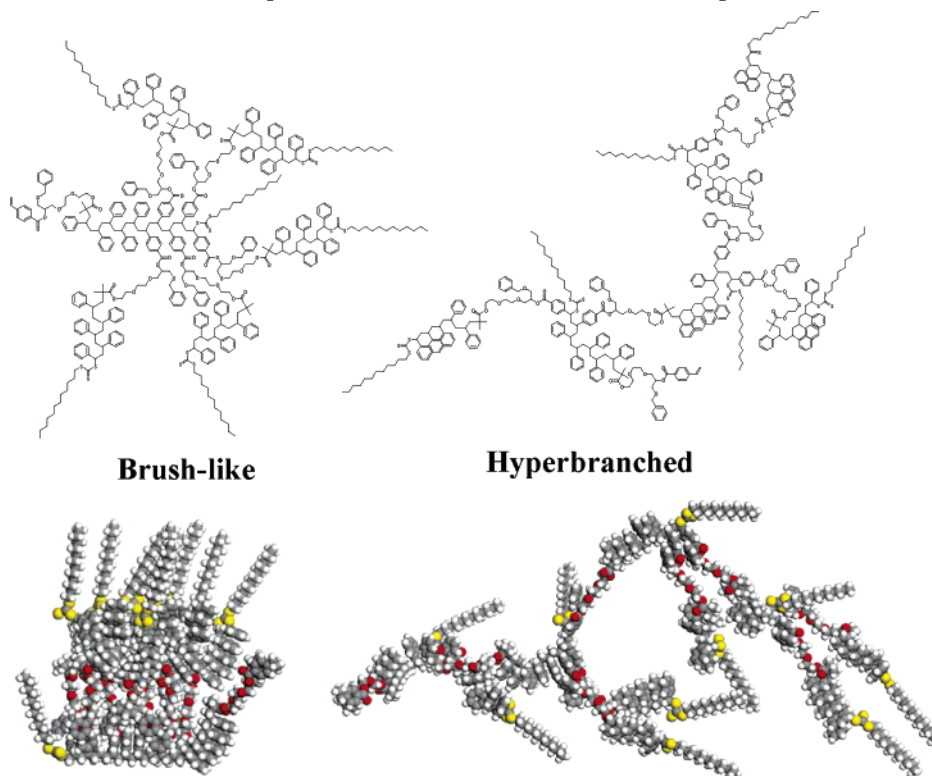
molecule, A_o, was calculated by the extrapolation of the steep rise in the surface pressure to a zero level in accordance with usual procedure (Table 3).[41] The hyperbranched copolymers **P1** and **P2** showed a steady increase in the surface pressure up to 40−50 mN/m upon compression of the monolayers below 3−4 nm²/molecules. In sharp contrast, **P3** with lower PS content showed an initial pressure increase for the surface areas around 11 nm² which was placed with a constant pressure of 10 mN/m

for surface areas below 7 nm² (Figure 9).

Figures 10 shows selected AFM images of the LB monolayers deposited on a bare silicon substrate at a surface pressure of 5 mN/m (expanded condensed state) for **P1** and **P2** hyperbranched copolymers. AFM exposed domain microstructure of the LB monolayers of the macroinitiators with domain heights of several nanometers. Uniform and continuous surface morphology was observed for monolayers from **P1** and **P2** at all surface pressures. AFM revealed very smooth surface with the microroughness in the range of 0.2−0.3 nm within a 1 × 1 μm² area. The thickness of these polymer monolayers was in the range of 1.7−2.8 nm measured by ellipsometry (Table 3).

LB monolayer fabricated from **P3** copolymer showed smooth morphology at very low pressure which is transformed to the well-developed domain morphology above first transition at the Langmuir isotherm (Figure 11). Further compression of the monolayer allowed merging of these domains and the formation of a smooth morphology again (Figure 11). However, the thickness of this layer doubled, indicating monolayer collapse and transition to a bilayer state at high surface pressure. This was not observed for hyperbranched copolymers with larger PS content (Table 3). Similar isotherms were obtained for the

Scheme 4. Chemical Structure and Corresponded Molecular Models of Two Possible Expected Architectures of the Polymer P3
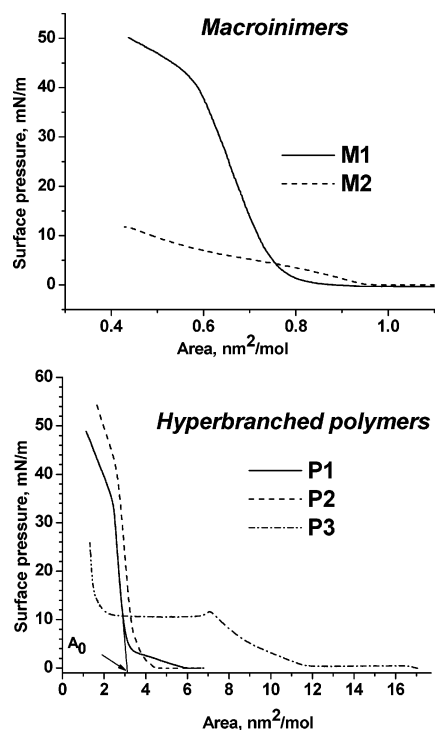
Figure 9. Pressure−area (π−A) isotherm of the TEG-PS macroinimers (top) and corresponded PEO−PS hyperbranched copolymers (bottom).

Table 3. Surface Properties of the Hyperbranched Copolymers

polymer	sample	area per molecule, nm^2			exptl thickness,[a] nm
		exptl	calcd		
			PEO	PS	
M1	TEG-PS	0.8	0.84	1.08	2.7
P1	TEG-PS (bulk)	3.2	2.5	3.24	2.7
P2	TEG-PS (DMF)	3.6	2.5	3.24	1.7
M2	TEG-PS−RAFT	0.9	0.84	0.3	2.0
P3	TEG-PS−RAFT	11.8	8.4	3.0	1.1[c]
					5.2 (10.3[b])
					11.8

[a] Obtained from ellipsometry. [b] Obtained from AFM cross-section in Figure 8. [c] The **P3** monolayer thickness was obtained for 5, 10, and 25 mN/m (from top to bottom).

monodendrons with oligo(ethylene glycol) tails.[70] It was shown that the surface stability of dendritic monolayer mostly depends on subtle balance between the relative sizes of the hydrophobic and hydrophilic groups.

Models of Surface Ordering. As is known, the surface behavior of hyperbranched copolymers should depend strongly upon the amphiphilic balance of the hydrophobic and hydrophilic fragments and the freedom of their reorganizations to adapt the proper orientation at the air−water interface which is constrained by the chemical architecture. Using two limiting molecular models described in Scheme 4, we analyzed the molecular arrangements at the air−water interface. By minimizing the total energy of the macromolecules, the molecular conformations of the polymers were optimized in order to maximize PEO fragment contact with water and distant positioning PS from the water (Figure 12).

Using two models of chemical architecture, the thickness of the monolayers were calculated and compared with actual ellipsometry data for different polymers (Table 3). We also estimated the limiting surface areas per molecule as expected from known surface areas for PEO monomeric unit (0.28 nm^2)[71] and for PS monomeric unit (0.06 nm^2)[34] and predicted chemical composition (Table 3). For two hyperbranched copolymers with
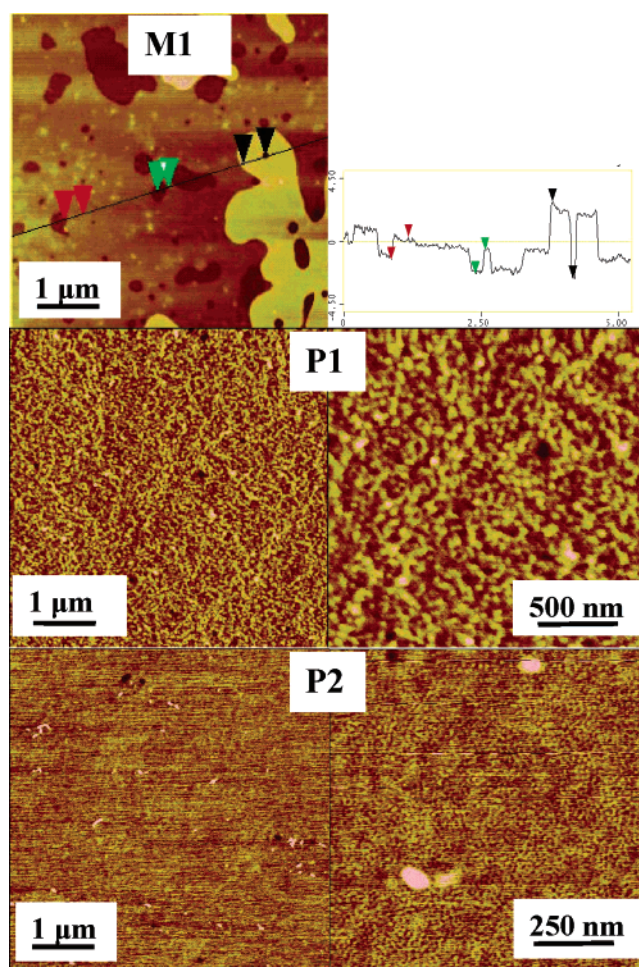

Figure 10. AFM topography of amphiphilic polymers: **M1** initiator (top, left) and its cross-sectional analysis), hyperbranched **P1**, **P2**, and **P3** polymers. Monolayers were deposited at surface pressure $\pi = 5$ mN/m. Scan areas are 5×5 μm^2 for all images on the left; on the right, they are 2×2 μm^2 for **P1** and 1×1 μm^2 for **P2**. Height is 10 nm for all images on the left and 3 nm for all images on the right.

predominant PS segments (**P1** and **P2**), the estimated thicknesses were close to those observed experimentally, suggesting that the PS hydrophobic fragments are oriented outward from the water surface and are not spread flatly. Indeed, for these hyperbranched copolymers with longer PS blocks, the experimental surface area per molecule was close to the minimum area estimated from chemical composition assuming PS as a limiting block for the monolayer compression in the condensed state (Table 3). Thus, for the hyperbranched copolymers with small content of the hydrophilic block and longer hydrophobic segments, PS or PEO chains are separated on different sides of the interface and serve as a "limiting" factor for the monolayer compression under different pressures similar to conventional star and linear block copolymers.[34,72] Other important factors, such as high PDI, a low degree of polymerization and the presence of considerable amount (10−15%) of unreacted macroinimers, also played a role in the formation of smooth monolayers of the hyperbranched polymers at the interfaces. We expect that a lower molecular weight fraction formed surface aggregates with variety of smaller sizes, which filled gaps between large scale aggregates formed by high molecular weight fraction, therefore lowering effective roughness of the resulting monolayers.

However, the hyperbranched copolymer **P3** with a comparable length of PS and PEO segments and considerably high degree of branching along with low PDI exhibited very different
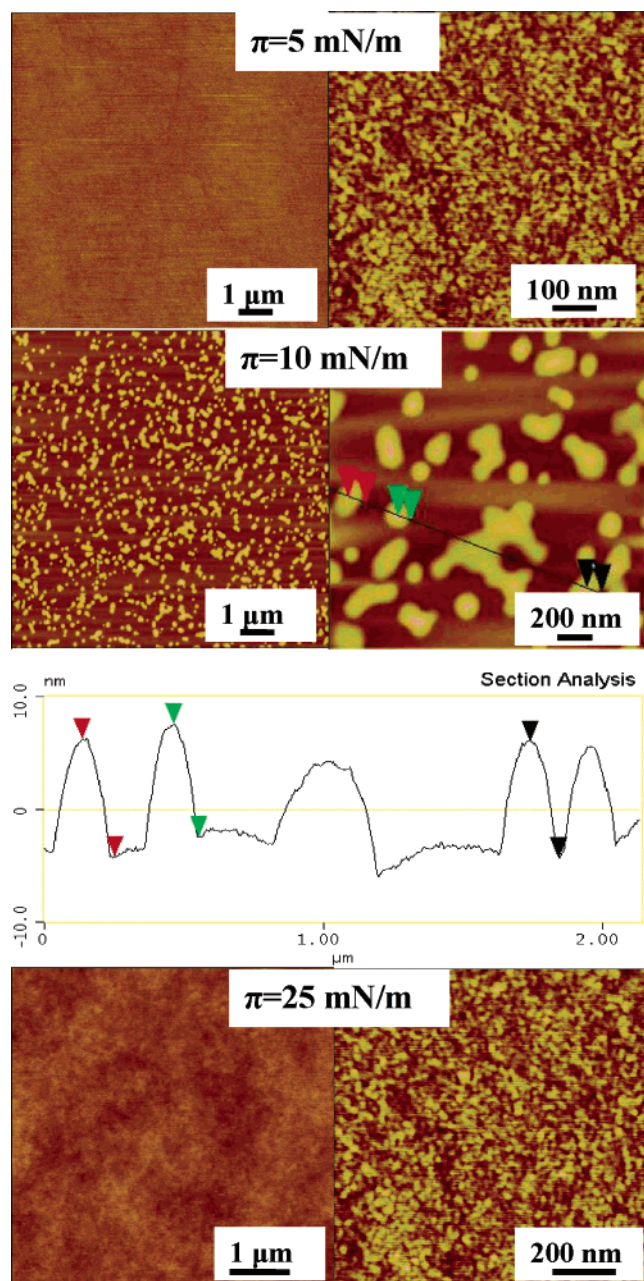
Figure 11. AFM topography of amphiphilic polymers **P3** polymer. Monolayers were deposited at different surface pressures. Scan areas are $10 \times 10\ \mu m^2$ for all images on the left, at the right $2 \times 2\ \mu m^2$, but $1 \times 1\ \mu m^2$ for $p = 5$ mN/m. Cross-section is for $p = 10$ mN/m. Height is 20 nm for all images on the left and 3 nm for all images on the right, but 20 nm for $p = 10$ mN/m.

surface behavior at the interfaces (Figure 12). The limiting factor for compression of the monolayer is the total surface area of *both segments* located at the water surface (Table 3). Dissimilar segments are not clearly separated into/out of water/air but rather formed a mixed uniform phase at the surface. This behavior is in striking contrast with conventional linear and star PEO−PS block copolymers (Figure 12, center) and indicates that a random chemical architecture of relatively short hydrophilic and hydrophilic fragments is responsible for a "mixed" interfacial structure. Thus, the presented hyperbranched model corresponds closely to the behavior observed for this copolymer (Figure 12 (right)). Correspondingly, the high compression results in the collapse of the mixed monolayer (rather than submerging PEO segments into the water subphase) and its transformation to the uniform bilayer.
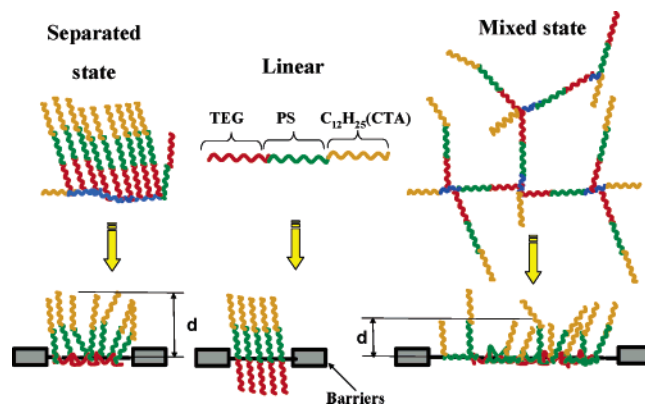

Figure 12. Two possible scenarios of state of the macromolecules at the air−water interface by comparison with linear block copolymer (center): left, separated hydrophobic and hydrophilic segments; right, mixed hydrophobic and hydrophilic segments confined to the water surface. Terminal chains added to reflect the presence of terminal alkyl ends.

Finally, we can conclude that the combination of both NMP and RAFT polymerizations provided a series of novel amphiphilic hyperbranched PEO−PS copolymers with chemical composition composed of mixed hydrophobic and hydrophilic segments but still possessing strong amphiphilic character. Furthermore, selective modifications of terminal initiating groups available in these hyperbranched copolymers can be further used to tune the chemical and physical properties without changes in hyperbranched cores as was demonstrated for star copolymers.[73] In addition, functional terminal groups can be used to further initiate polymerization of a variety of monomers which will result in new highly branched functional star polymers.

References and Notes

(1) Roovers, J. In *Encyclopedia of Polymer Science and Engineering*, 2nd ed.; Kroschwitz, J. I., Ed.; Wiley-Interscience: New York, 1985; Vol. 2, 478.
(2) Mishra, M. K., Kobayashi, S., Eds. *Star and Hyperbranched Polymers*; Marcel Dekker: New York, 1999; Vol. 53, 350.
(3) Fischer, M.; Vogtle, F. *Angew. Chem., Int. Ed. Engl.* **1999**, *38*, 885.
(4) Tomalia, D. A.; Naylor, A. M.; Goddard, W. A. *Angew. Chem., Int. Ed. Engl.* **1990**, *29*, 138.
(5) Fréchet, J. M. J. *Science* **1994**, *263*, 1710.
(6) Kim, Y. H. *J. Polym. Sci., Part A: Polym. Chem.* **1998**, *36*, 1685.
(7) Newkome, G. R., Moorefield, C. N., Vogtle, F., Eds. *Dendritic Molecules*, VCH: Weinheim, Germany, 1996; 261.
(8) Yan, D.; Zhou, Y.; Hou, J. *Science* **2004**, *303*, 65.
(9) Jones, M.-C.; Ranger, M.; Leroux, J.-C. *Bioconjugate Chem.* **2003**, *14*, 774.
(10) Isayeva, I. S.; Yankovski, S. A.; Kennedy, J. P. *Polym. Bull. (Berlin)* **2002**, *48*, 475.
(11) Xiea, H.-Q.; Xieb, D. *Prog. Polym. Sci.* **1999**, *24*, 275.
(12) Voulgaris, D.; Tsitsilianis, C.; Esselink, F. J.; Hadziioannou, G. *Polymer* **1998**, *39*, 6429.
(13) Narrainen, A. P.; Pascual, S.; Haddleton, D. M. *J. Polym. Sci., Part A: Polym. Chem.* **2002**, *40*, 439.
(14) Voulgaris, D.; Tsitsilianis, C. *Macromol. Chem. Phys.* **2001**, *202*, 3284.
(15) (a) Ornatska, M.; Bergman, K. N.; Rybak, B.; Peleshanko, S.; Tsukruk, V. V. *Angew. Chem.* **2004**, *43*, 5246. (b) Ornatska, M.; Peleshanko, S.; Genson, K. L.; Rybak, B.; Bergman, K. N.; Tsukruk, V. V. *J. Am. Chem. Soc.* **2004**, *126*, 9675. (c) Zhai, X.; Peleshanko, S.; Klimenko, N. S.; Genson, K. L.; Vortman, M. Ya.; Shevchenko, V. V.; Vaknin, D.; Tsukruk, V. V. *Macromolecules* **2003**, *36*, 3101. (d) Shulha, H.; Zhai, X.; Tsukruk, V. V. *Macromolecules* **2003**, *36*, 2825. (e) Tsukruk, V. V.; Shulha, H.; Zhai, X. *Appl. Phys. Lett.* **2003**, *82*, 907.

(16) Ornatska, M.; Peleshanko, S.; Rybak, B.; Holzmueller, J.; Tsukruk, V. V. *Adv. Mater.* **2004**, *16*, 2206.

(17) Rybak, B. M.; Bergman, K. N.; Ornatska, M.; Genson, K. L.; Tsukruk, V. V. *Langmuir* **2006**, *22*, 1027.

(18) Boyce, J. R.; Shirvanyants, D.; Sheiko, S. S.; Ivanov, D. A.; Qin, S.; Boerner, H.; Matyjaszewski, K. *Langmuir* **2004**, *20*, 6005.

(19) Lord, S. J.; Sheiko, S. S.; LaRue, I.; Lee, H.; Matyjaszewski, K. *Macromolecules* **2004**, *37*, 4235.

(20) Kanaoka, S.; Kanaoka, S.; Nakata, S.; Yamaoka, H. *Macromolecules* **1992**, *25*, 6414.

(21) Kanaoka, S.; Sawamoto, M.; Higashimura, T. *Macromolecules* **1993**, *26*, 254.

(22) Genson, K. L.; Hoffman, J.; Teng, J.; Zubarev, E. R.; Vaknin, D.; Tsukruk, V. V. *Langmuir* **2004**, *20*, 9044.

(23) (a) Luzinov, I.; Minko, S.; Tsukruk, V. V. *Prog. Polym. Sci.* **2004**, *29*, 635. (b) Tsukruk, V. V. *Prog. Polym. Sci.* **1997**, *22*, 247.

(24) Holzmueller, J.; Genson, K. L.; Park, Y.; Yoo, Y.-S.; Park, M.-H.; Lee, M.; Tsukruk, V. V. *Langmuir* **2005**, *21*, 6392.

(25) Kanaoka, S.; Nakata, S.; Yamaoka, H. *Macromolecules* **2002**, *35*, 4564.

(26) Herman, D. S.; Kinning, D. J.; Thomas, E. L.; Fetters, L. J. *Macromolecules* **1987**, *20*, 2940.

(27) Tselikas, Y.; Hadjichristidis, N.; Lescanec, R. L.; Honeker, C. C.; Wohlgemuth, M.; Thomas, E. L. *Macromolecules* **1996**, *29*, 2290.

(28) Pochan, D. J.; Gido, S. P.; Pispas, S.; Mays, J. W.; Ryan, A. J.; Fairclough, P. A.; Hamley, I. W.; Terrill, N. J. *Macromolecules* **1996**, *29*, 5091.

(29) Pochan, D. J.; Gido, S. P.; Pispas, S.; Mays, J. W. *Macromolecules* **1996**, *29*, 5099.

(30) Francis, R.; Taton, D.; Logan, J. L.; Masse, P.; Gnanou, Y.; Duran, R. S. *Macromolecules* **2003**, *36*, 8253.

(31) Francis, R.; Skolnik, A. M.; Carino, S. R.; Logan, J. L.; Underhill, R. S.; Angot, S.; Taton, D.; Gnanou, Y.; Duran, R. S. *Macromolecules* **2002**, *35*, 6483.

(32) Matmour, R.; Lepoittevin, B.; Joncheray, T. J.; El-khouri, R. J.; Taton, D.; Duran, R. S.; Gnanou, Y. *Macromolecules* **2005**, *38*, 5459.

(33) Logan, J. L.; Masse, P.; Gnanou, Y.; Taton, D.; Duran, R. S. *Langmuir* **2005**, *21*, 7380.

(34) Peleshanko, S.; Jeong, J.; Gunawidjaja, R.; Tsukruk, V. V. *Macromolecules* **2004**, *37*, 6511.

(35) Peleshanko, S.; Gunawidjaja, R.; Jeong, J.; Shevchenko, V. V.; Tsukruk, V. V. *Langmuir* **2004**, *20*, 9423.

(36) Kim, Y. H.; Webster, O. W. *Macromolecules* **1992**, *25*, 5561.

(37) Brenner, A. R.; Voit, B. I. *Macromol. Chem. Phys.* **1996**, *197*, 2673.

(38) (a) Hawker, C. J.; Fréchet, J. M. J.; Grubbs, R. B.; Dao, J. *J. Am. Chem. Soc.* **1995**, *117*, 10763. (b) Grubbs, R. B.; Hawker, C. J.; Dao, J.; Fréchet, J. M. J. *Angew. Chem., Int. Ed. Engl.* **1997**, *36*, 270.

(39) Gauthier, M.; Tichagwa, L.; Downey, J. S.; Gao, S. *Macromolecules* **1996**, *29*, 519.

(40) Weberskirch, R.; Hettich, R.; Nuyken, O.; Schmaljohann, D.; Voit, B. *Macromol. Chem. Phys.* **1999**, *200*, 863.

(41) Velichkova, R. S.; Christova, D. C. *Prog. Polym. Sci.* **1995**, *20*, 819.

(42) Sunder, A.; Hanselmann, R.; Frey, H.; Mülhaupt, R. *Macromolecules* **1999**, *32*, 4240.

(43) Sunder, A.; Frey, H.; Mülhaupt, R. *Macromolecules* **2000**, *33*, 309.

(44) Knischka, R.; Lutz, P. J.; Sunder, A.; Mülhaupt, R.; Frey, H. *Macromolecules* **2000**, *33*, 315.

(45) Maier, S.; Sunder, A.; Frey, H.; Mülhaupt, R. *Macromol. Rapid Commun.* **2000**, *21*, 226.

(46) Gaynor, S. G.; Edelman, S.; Matyjaszewski, K. *Macromolecules* **1996**, *29*, 1079.

(47) Cheng, G.; Simon, P. F. W.; Hartenstein, M.; Müller, A. H. E. *Macromol. Rapid Commun.* **2000**, *21*, 846.

(48) Peeters, J. W.; Palmans, A. R. A.; Meijer, E. W.; Koning, C. E.; Heise, A. *Macromol. Rapid Commun.* **2005**, *26*, 684.

(49) Nomura, R.; Matsuno, T.; Endo, T. *Polym. Bull. (Berlin)* **1999**, *42*, 251.

(50) Cheng, C.; Wooley, K. L.; Khoshdel, E. *J. Polym. Sci., Part A: Polym Chem.* **2005**, *43*, 4754.

(51) Jin, M.; Lu, R.; Bao, C.; Xu, T.; Zhao, Y. *Polymer* **2004**, *45*, 1125.

(52) (a) Liu, B.; Kazlauciunas, A.; Guthrie, J. T.; Perrier, S. *Macromolecules* **2005**, *38*, 2131. (b) Liu, B.; Kazlauciunas, A.; Guthrie, J. T.; Perrier, S. *Polymer* **2005**, *46*, 6293.

(53) Perrier, S.; Takolpuckdee, P.; Mars, C. A. *Macromolecules* **2005**, *38*, 2033.

(54) Matyjaszewski, K.; Miller, P. J.; Pyun, J.; Kickelbick, G.; Diamanti, S. *Macromolecules* **1999**, *32*, 6526.

(55) Lai, J. T.; Filla, D.; Shea, R. *Macromolecules* **2002**, *35*, 6754.

(56) Greene, T. W.; Wuts, P. G. M. *Protective Groups in Organic Synthesis.* 3rd ed.; Wiley-Interscience: New York, 1999; p 779.

(57) (a) Tsukruk, V. V. *Rubber Chem. Technol.* **1997**, *70*, 430. (b) Tsukruk, V. V.; Reneker, D. H. *Polymer* **1995**, *36*, 1791.

(58) Chaudhary, S. K.; Hernandez, O. *Tetrahedron Lett.* **1979**, *20*, 99.

(59) Ramakrishnan, A.; Dhamodharan, R. *Macromolecules* **2003**, *36*, 1039.

(60) Matyjaszewski, K.; Woodworth, B. E.; Zhang, X.; Gaynor, S. G.; Metzner, Z. *Macromolecules* **1998**, *31*, 5955.

(61) Bon, S. A. F.; Steward, A. G.; Haddleton, D. M. *J. Polym. Sci., Part A: Polym. Chem.* **2000**, *38*, 2678.

(62) Pouchert, C. J.; Behnke, J. *The Aldrich Library of ^{13}C and ^1H FT-NMR Spectra*; Aldrich Chemical: Milwaukee, WI, 1992.

(63) Simon, P. F. W.; Müller, A. H. E. *Macromol. Theory Simul.* **2000**, *9*, 621.

(64) Xia, J.; Hui, Y.-Z. *Chem. Pharm. Bull.* **1999**, *47*, 1659.

(65) Zheng, G.; Pan, C. *Polymer* **2005**, *46*, 2802.

(66) Stenzel, M. H.; Davis, T. P.; Fane, A. G. *J. Mater. Chem.* **2003**, 2090.

(67) (a) Pitsikalis, M.; Pispas, S.; Mays, J. W.; Hadjichristidis, N. *Adv. Polym. Sci.* **1998**, *135*, 1. (b) Hadjichristidis, N.; Pispas, S.; Pitsikalis, M.; Iatrou, H.; Vlahos, C. *Adv. Polym. Sci.* **1999**, *142*, 71.

(68) (a) Brochard-Wyart, F.; de Gennes, P. G. *C. R. Acad. Sci. Paris* **1996**, *323*, 473. (b) Gay, C.; Raphaël, E. *Adv. Colloid Interface Sci.* **2001**, *94*, 229.

(69) Ulman, A. *Introduction to Ultrathin Organic Films*, Academic Press: San Diego, CA, 1991; p 442.

(70) Kampf, J. P.; Frank, C. W.; Malmstrom, E. E.; Hawker, C. J. *Langmuir* **1999**, *15*, 227.

(71) Cox, J. K.; Yu, K.; Constantine, B.; Eisenberg, A.; Lennox, R. B. *Langmuir* **1999**, *15*, 7714.

(72) a) Kumaki, J. *Macromolecules* **1988**, *21*, 749. (b) Kawaguchi, M.; Sauer, B. B.; Yu, H. *Macromolecules* **1989**, *22*, 1735.

(73) Gunawidjaja, R.; Peleshanko, S.; Tsukruk, V. V. *Macromolecules* **2005**, *38*, 8765.